BIOCELL
2019 43(4): 271-283

Tech Science Press

An extract of *Hypericum perforatum* induces wound healing through inhibitions of Ca^{2+} mobilizations, mitochondrial oxidative stress and cell death in epithelial cells: Involvement of TRPM2 channels

Fuat USLUSOY[1]; Mustafa NAZIROĞLU[2,3,*]

[1] Department of Plastic Reconstructive and Aesthetic Surgery, Faculty of Medicine, Suleyman Demirel University, Isparta, Turkey
[2] Neuroscience Research Center, Suleyman Demirel University, Isparta, Turkey
[3] Drug Discovery Unit, BSN Health, Analysis and Innovation Ltd. Inc. Teknokent, Isparta, Turkey

Key words: Apoptosis, *Hypericum perforatum*, Oxidative stress, TRPM2 channel, Wound

Abstract: The wound is induced by several mechanical and metabolic factors. In the etiology of the wound recovery, excessive oxidative stress, calcium ion (Ca^{2+}) influx, and apoptosis have important roles. Ca^{2+}-permeable TRPM2 channel is activated by oxidative stress. Protective roles of *Hypericum perforatum* extract (HP) on the mechanical nerve injury-induced apoptosis and oxidative toxicity through regulation of TRPM2 in the experimental animals were recently reported. The potential protective roles in HP treatment were evaluated on the TRPM2-mediated cellular oxidative toxicity in the renal epithelium (MPK) cells. The cells were divided into three groups as control, wound, and wound + HP treatment (75 μM for 72 h). Wound diameters were more importantly decreased in the wound+HP group than in the wound group. In addition, the results of laser confocal microscopy analyses indicated protective roles of HP and TRPM2 antagonists (N-(p-Amylcinnamoyl) anthranilic acid and 2-aminoethyl diphenylborinate) against the wound-induced increase of Ca^{2+} influx and mitochondrial ROS production. The wound-induced increase of early (annexin V-FITC) apoptosis and late (propidium iodide) apoptosis were also decreased in the cells by the HP treatment. In conclusion, HP treatment acted protective effects against wound-mediated oxidative cell toxicity and apoptosis through TRPM2 inhibition. These effects may be attributed to their potent antioxidant effect.

List of Abbreviations

$[Ca^{2+}]i$, intracellular free Ca^{2+} concentration
2-APB, 2-aminoethyl diphenylborinate
ACA, N-(p-amylcinnamoyl)anthranilic acid
ADPR, ADP-ribose
aV-FITC, Annexin V-FITC
DHR123, Dihydro-rhodamine 123
HP, *Hypericum perforatum* extract
JC-1, 5,5' ,6,6' -tetrachloro-1,1' ,3,3' tetra ethylbenzimidazolyl carbocyanine iodide
MMP, mitochondrial membrane depolarization
PI, propidium iodide
ROS, reactive oxygen species
TRPM2, transient receptor potential melastatin 2
VGGC, voltage gated calcium channel

Introduction

A wound is a kind of tissue injury and it was induced in the skin by several factors such as mechanical injury, burn, and diabetes (Działo *et al*., 2016; Li *et al*., 2019). The epithelial cells in the skin induce a barrier to wound through activation and inhibition of several molecular mechanisms. One signal that has a ubiquitous response in epithelial wound healing is the release of ATP (Yin *et al*., 2007). After the wound injury, extracellular ATP binds to purinoreceptors/cation channels and activates excessive calcium ion (Ca^{2+}) influx and mitochondrial membrane depolarization (MMP) (Adinolfi *et al*., 2009; Takada *et al*., 2017; Lee *et al*., 2019). In turn, the overload Ca^{2+} influx induces excessive mitochondrial reactive oxygen species (ROS) production and cell death (Nazıroğlu, 2012). However, the Ca^{2+} influx response is mimicked in a wound and injury medium by using the voltage calcium channel (VGCC) blockers such as diltiazem, nifedipine, and verapamil (Dubé *et al*., 2012; Nazıroğlu *et al*., 2013; Ashkani-Esfahani *et al*., 2016). *Hypericum perforatum* extract (HP) has also VGCC blocker effects, as well as the verapamil and diltiazem in neurons, neutrophils and epithelial cells (Nazıroğlu *et al*., 2014a; Takada *et al*., 2017), and it may induce wound healing action through regulation of excessive Ca^{2+} influx. To understand how epithelial cells, give the response to HP treatment after wound injury, the Ca^{2+} influx and cell death processes need to be studied.

*Address correspondence to: Mustafa NAZIROĞLU, mustafanaziroglu@sdu.edu.tr

It is well known that the accumulation of Ca^{2+} is the main reason for several physiologic and pathophysiologic functions, including wound recovery and cell death (Lee *et al*., 2019). Activations of several channels such as VGCC and chemical channels induce Ca^{2+} influxes. In addition to the VGCC and chemical channels, the transient receptor potential (TRP) superfamily was discovered within the last decades (Clapham, 2003; Nazıroğlu, 2012). The TRP superfamily members have several positive effects on skin biology and pathophysiology (Caterina and Pang, 2016). A member of the TRP superfamily is the TRP melastatin 2 (TRPM2) channel. TRPM2 channel is activated by ADP-ribose (ADPR) and oxidative stress (Hara *et al*., 2002; Nazıroğlu and Lückhoff, 2008). It was recently reported that apoptosis was induced in epithelial cells by TRPM2 activation (Liu *et al*., 2018). In addition to the wound injury-induced TRPM2 channel activation, several studies suggested that mitochondrial oxidative stress was also one of the reasons for causing wound injury and cell toxicity through activation of TRPM2 channels (Nazıroğlu *et al*., 2013; Kang *et al*., 2018). Hence, it seems that the TRPM2 channel activation has a main potential role in wound injury or recovery.

The 'St. John's wort' *Hypericum perforatum* is a well-known traditional plant, and it has been used in the treatment of several diseases such as depression, inflammatory, and skin diseases (Meinke *et al*., 2012; Nazıroğlu, 2016). The main components of *H. perforatum* are hyperforin, flavonoids, hypericin, and their anti-apoptosis and antioxidant properties through inhibition of TRPM2 channel were reported in neuropathic pain, neutrophil activation and mechanical brain injury (Nazıroğlu *et al*., 2014a, 2014b, 2014c; Uslusoy *et al*., 2017). In addition, involvements of HP through inhibition of TRPM2 channels in the mechanical sciatic nerve and spinal cord injuries were recently reported (Pogatzki-Zahn *et al*., 2005; Özdemir *et al*., 2016; Uslusoy *et al*., 2017; Uslusoy *et al*., 2019). Involvement of HP through inhibition of TRPM2 channel in the recovering skin injury has not been clarified yet, although results of recent studies indicated protective roles of HP treatments through inhibition of oxidative stress on diabetic surgical wound (Altıparmak and Eskitaşçıoğlu, 2018) and burn wound healing (Vafi *et al*., 2016) in rats. It was also reported that HP and hyperforin induced a proliferative action toward keratinocytes through activation of TRPC6 (Wolfle *et al*., 2004; Takada *et al*., 2017). HP may have also a modulatory role in TRPM2 channel activation in the wound healing process of epithelial cells.

In order to gain further insight into the mechanisms of actions of HP treatments, current study investigated the effect of HP on wound healing in cell culture model, and further explored the influences of HP incubation on apoptosis in vitro and its possible Ca^{2+} signaling through TRPM2 channel activation. The results from current study may provide further explanation for the effect of HP applications in the healing skin wound.

Materials and Methods

Reagents

Dimethyl sulfoxide (DMSO), dihydro-rhodamine 123 (DHR 123), and N-methyl-D-glucamine (NMDG) were purchased from Sigma Aldrich (St. Louis, MO, USA). N-(p-Amylcinnamoyl) anthranilic acid (ACA) and 2-aminoethyl diphenylborinate (2-APB), as two TRPM2 blockers, were purchased from Santa Cruz (Istanbul, Turkey). Fluo-3, propidium iodide (PI) and Annexin V-FITC (aV-FITC) were purchased from Calbiochem Inc. (Darmstadt, Germany) and Cell Signaling (Istanbul, Turkey), respectively. 5,5 ′ ,6,6 ′ -tetrachloro-1,1 ′ ,3,3 ′ tetra ethylbenzimidazolyl carbocyanine iodide (JC-1) was purchased from Molecular Probes Inc. (Eugene, OR, USA). Fetal bovine serum (FBS), DMEM, and Ham's F12 cell culture media were purchased from Thermo Fischer Sci. Inc. (Istanbul, Turkey).

Hypericum perforatum extract (HP)

We used commercial *H. perforatum* extract (HP) from Indena Inc. (Indena Industria Derivati Naturali, S.p.A. Viale Ortles, Milan, Italy) (Özdemir *et al*., 2016; Uslusoy *et al*., 2017). Contents of total hypericin, flavonoids, and hyperforin in the extract were analyzed by the company, and their rates were 0.10-0.30, 6.0, and 6.0%, respectively. The HP was dissolved in DMSO (1.0%) before dilution with the cell culture growth medium.

Cell culture

In the current study, we used mice renal epithelial mpkCCD$_{c14}$ (MPK) cells, because we recently found high TRPM2 expression levels in the cells (Nazıroğlu *et al*., 2019). The cells were gifts from Prof. Dr. Franziska Theilig (Christian-Albrechts-University of Kiel, Kiel, Germany). The MPK cells were cultured in defining the medium as described previously (Polzin *et al*., 2010). In brief, the growth medium was composed of DMEM (45%) and Ham's F12 (45%). Remaining 10% of the medium contained 10% FBS, antibiotics, and the appropriate supplements.

The cells were grown in a 5% CO_2/95% air atmosphere at 37°C. The cells were either treated with HP. The used concentrations were indicated in the figure legends. In some experiments, specific TRPM2 blockers [ACA (25 μM) and 2-APB (100 μM)] and and activator (H_2O_2 and 1 mM) were applied additionally to the culture media used.

Wound induction in the epithelial MPK cells

The cells were seeded in 35 mm glass-bottom dishes (Mattek Corporation Inc., Ashland, MA, USA). The cells totally covered the glass bottom dishes within 3 days. Then, 400-500 μm wounds were induced in the middle of each dish by using a sterile yellow pipette tip. After incubation with HP doses, the cells were kept in the cell culture medium.

Detection of non-toxic doses of HP on the wound healing in the MPK cells and groups

There was no report on the non-toxic doses of HP in the MPK cells. We detected non-toxic doses of HP on the wound healing in the MPK cells**.** In several in vitro experiments, HP doses were used between 5 and 125 μM for 24-72 h (Schmitt *et al*., 2006; Nazıroğlu *et al*., 2014a; Oliveira *et al*., 2016). For the reasons, the wound-induced cells were incubated with HP doses (0, 5, 10, 25, 50, 75, 100, and 125 μM). At the end of the third day, bride filed records were performed.

Groups

The cells were mainly divided into three groups: (1) *Control group*: The cells were not incubated with HP, but they were kept in a flask containing the same cell culture medium and conditions for 72 h; (2) *Wound group*: The cells in the group kept 72 h in the cell same culture condition after induction of wound (Takada *et al*., 2017); and (3) *Wound+HP* group: After induction of wound, the cells in the group were kept in the cell culture medium for 30 min, and then they were treated with HP (75 μM) for a further period of 72 h.

In the laser confocal microscopy analyses, the cells were seeded in 35 mm glass-bottom dishes**.** In patch-clamp experiments, the cells were directly taken from the dishes to the patch chamber.

Bride field records in laser confocal microscope

For taking bride field records, Axiocam 702 mono high-performance CMOS microscope camera (2.3 megapixels and a sensor size of 1/1.2 was used. The camera was adapted to the laser confocal microscope (LSM 800) by the manufacturer (Zeiss, Ankara, Turkey). The wound diameters of the injuries were measured by using ZEN program (Zeiss Inc.) and the mean values were expressed as μm.

Measurement of intracellular free Ca^{2+}($[Ca^{2+}]_i$) fluorescence intensity through TRPM2 activation

Changes in the wound-induced TRPM2 channel activation in the MPK cell samples were detected by using a laser confocal microscope. Changes in the concentration of Ca^{2+} fluorescence intensity in the 10–15 cells MPK cells were measured in the ZEN program (Zeiss) by using 1 μM Fluo-3 Ca^{2+} indicator fluorescent dye (Baş *et al*., 2019). The Fluo-3 was excited in the confocal microscope fitted with a 40X oil objective (Zeiss) by a 488 nm argon. The cells were pretreated with ACA (25 μM) and 2-APB (100 μM) to inhibit Ca^{2+} entry before stimulation of H_2O_2 (1 mM). The results of Fluo-3 in 20 mm^2 of cytosol were expressed as the mean fluorescence intensity as arbitrary units per cell.

Detection of intracellular reactive oxygen species (ROS) production and mitochondrial membrane potential (MMP) levels

DHR123 is an indicator of intracellular ROS changes in laser confocal microscope, and it becomes fluorescent upon oxidation to yield rhodamine 123 (Rh 123) (Joshi and Bakowska, 2011; Oz *et al*., 2017). One common indicator in the MMP is JC-1 fluorescent dye. For measurement of ROS and MMP in the cells, we used DHR123 and JC-1 dyes as described in previous studies (Joshi and Bakowska, 2011; Keil *et al*., 2011; Oz *et al*., 2017; Ertilav *et al*., 2019). The cell samples were analyzed in the laser confocal microscopy. JC-1 (505 nm excitation, 535 emission) and DHR123 (514 nm excitation, 570 emission) were excited at 488 nm. The results of DHR123 and JC-1 in 20 μm^2 of cytosol were expressed as the mean fluorescence intensity as arbitrary unit/cell.

.

*Annexin V-FITC (*aV-FITC*) and propidium iodide (PI) assays by laser confocal microscope*

The protective effects of wound-induced apoptosis were determined by the laser confocal microscope (LSM-800) using the annexin V (V-FITC) and PI apoptosis dyes, according to the manufacturer's instructions (Santa Cruz Biotechnology). PI is a fluorochrome for the detection of apoptotic cells. The PI is a membrane-impermeable dye. Hence, the state of the cell determines the ability of PI staining to distinguish between viable and late apoptotic cells (Pariente *et al*., 2018). At the end of the HP treatment (72 h), treated or resting cells were incubated with 250 μL binding buffer containing 5 μl of V-FITC for 15 min at room temperature in dark and then they were washed twice with 1X PBS, and finally the cells were incubated with 250 μL binding buffer containing 10 μL of PI for 15 min at room temperature in dark. After washing the PI dye with 1X PBS, the samples in 250 μL 1X BPS with Ca^{2+} (1.2 mM) were analyzed by the laser confocal microscopy fitted with a 40X oil objective. The emission of PI was detected at 617 nm (red) as described in a recent study (Ertilav *et al*., 2019). The results of aV-FITC and PI were expressed as the mean fluorescence intensity as arbitrary unit/cell.

Electrophysiology

Whole-cell recordings at room temperature were performed by using an EPC 10 USB amplifier equipped with a personal computer with PATCHMASTER software (HEKA, Lamprecht, Germany). Details of the standard intracellular and extracellular solutions were given in previous studies (Nazıroğlu *et al*., 2013; Özdemir *et al*., 2016). For preparing Na^+ free extracellular buffer, 150 mM $NMDG^+$ was used instead of Na^+, and the titration was performed with HCl. It is well-known that the TRPM2 channel is activated in the presence of high intracellular Ca^{2+} (McHugh *et al*., 2003). Therefore, the intracellular Ca^{2+} concentration was adjusted to 1 μM (0.886 mM Ca^{2+}, 1 mM Cs-EGTA) instead of 0.1 μM. For the stimulation of TRPM2 channels, ADPR was used, and its stock solution (100 mM) was prepared in sterile distilled water. For inhibition of TRPM2 currents, ACA (25 μM) was used. The current-voltage relations were obtained during voltage ramps from -150 to +150 mV and back to -150 mV applied over 200 ms. The holding potential was clamped to -60 mV. The analysis of the maximal current amplitudes (pA) in a cell were calculated by dividing the cell capacitance (pF) to measure the cell surface. The patch-clamp results were expressed as the current density (pA/pF) in the cells.

Statistical analysis

Statistical analysis was performed using the statistical software SPSS 20.0 (SPSS Inc. Chicago, Illinois, USA). All data were presented as mean ± standard deviation (mean ± SD) and analyzed using post hoc least significant difference (LSD) test. For significant values, a Mann-Whitney *U*-test was utilized. Statistically significant values were those with a p-value ≤ 0.05.

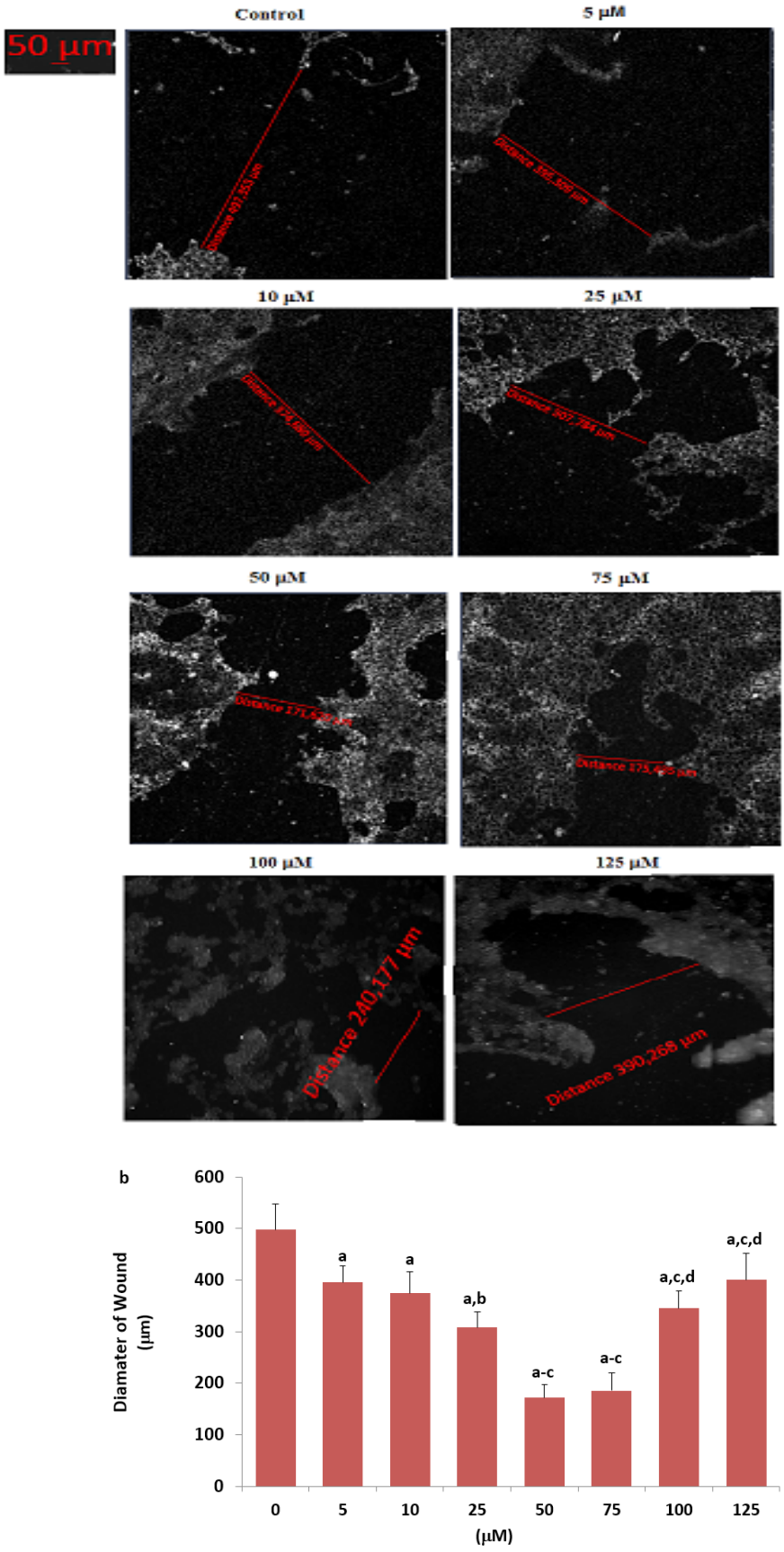

FIGURE 1. ***Hypericum perforatum*** **extract (HP) modulates wound healing in the MPK cells dose dependently**. (n = 8, mean ± SD). The wounds were induced in the MPK cells by using the sterile yellow pipette tip. Then the cells were incubated with 5, 10, 25, 50, 75, 100, and 125 µM of HP for 72 h. Then, bride field images of the injuries in the wound groups were taken in laser confocal microscope by using the high-performance camera (Axiocam 702 mono). The samples were analyzed by the laser confocal microscopy fitted with a 10X objective (a). Changes in the diameter of wounds were shown by columns (b). ([a] $p \leq 0.001$ versus zero; [b] $p \leq 0.001$ *vs.* 5 and 10 µM groups; [c] $p \leq 0.001$ *vs.* 25 µM group; [d] $p \leq 0.001$ *vs.* 50 and 75 µM groups).

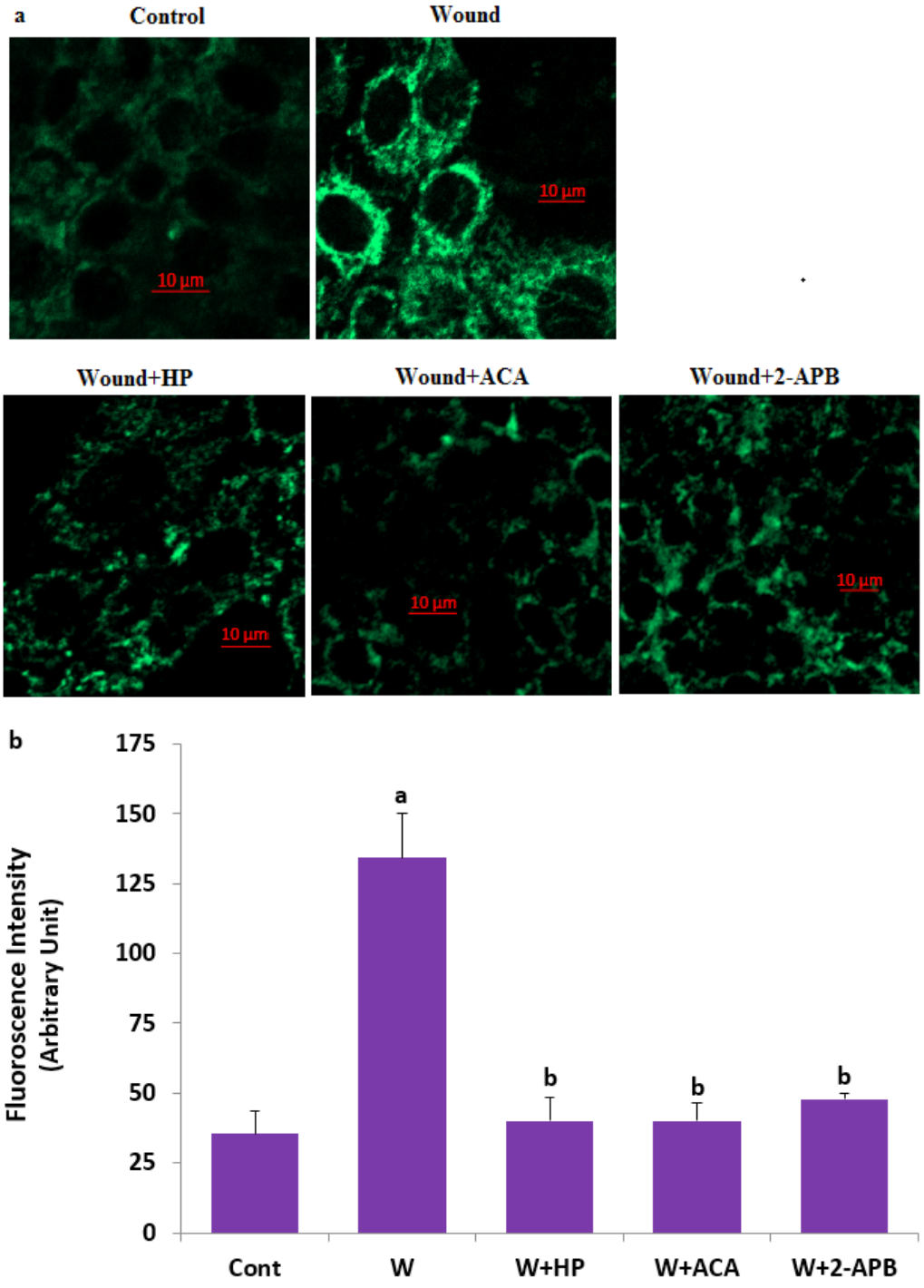

FIGURE 2. ***Hypericum perforatum*** **extract (HP) and TRPM2 channel blockers (ACA and 2-APB) attenuated wound (W)-induced increase of $[Ca^{2+}]_i$ concentration in the MPK cells**. Control, wound (W), and W + HP (75 µM) cells were kept in the cell culture conditions for 72 h. Some cells in the W group were further incubated with ACA (25 µM) and 2-APB (100 µM) for 30 min. The cells were stained with Fluo-3 calcium dye for one hour and mean ± SD of fluorescence in 20 mm^2 of the cells as arbitrary unit are presented; n = 15-20 independent experiments. The cells in the five groups were extracellularly stimulated by H_2O_2 (1 mM for 10 min). The samples were analyzed by the laser confocal microscopy fitted with a 40X oil objective. (A) Images of the Ca^{2+} fluorescence intensity in the five groups. Changes of the Ca^{2+} fluorescence intensity in the five groups were also shown by columns (B). ($^a p \leq 0.001$ *vs.* control group; $^b p \leq 0.001$ *vs.* W group).

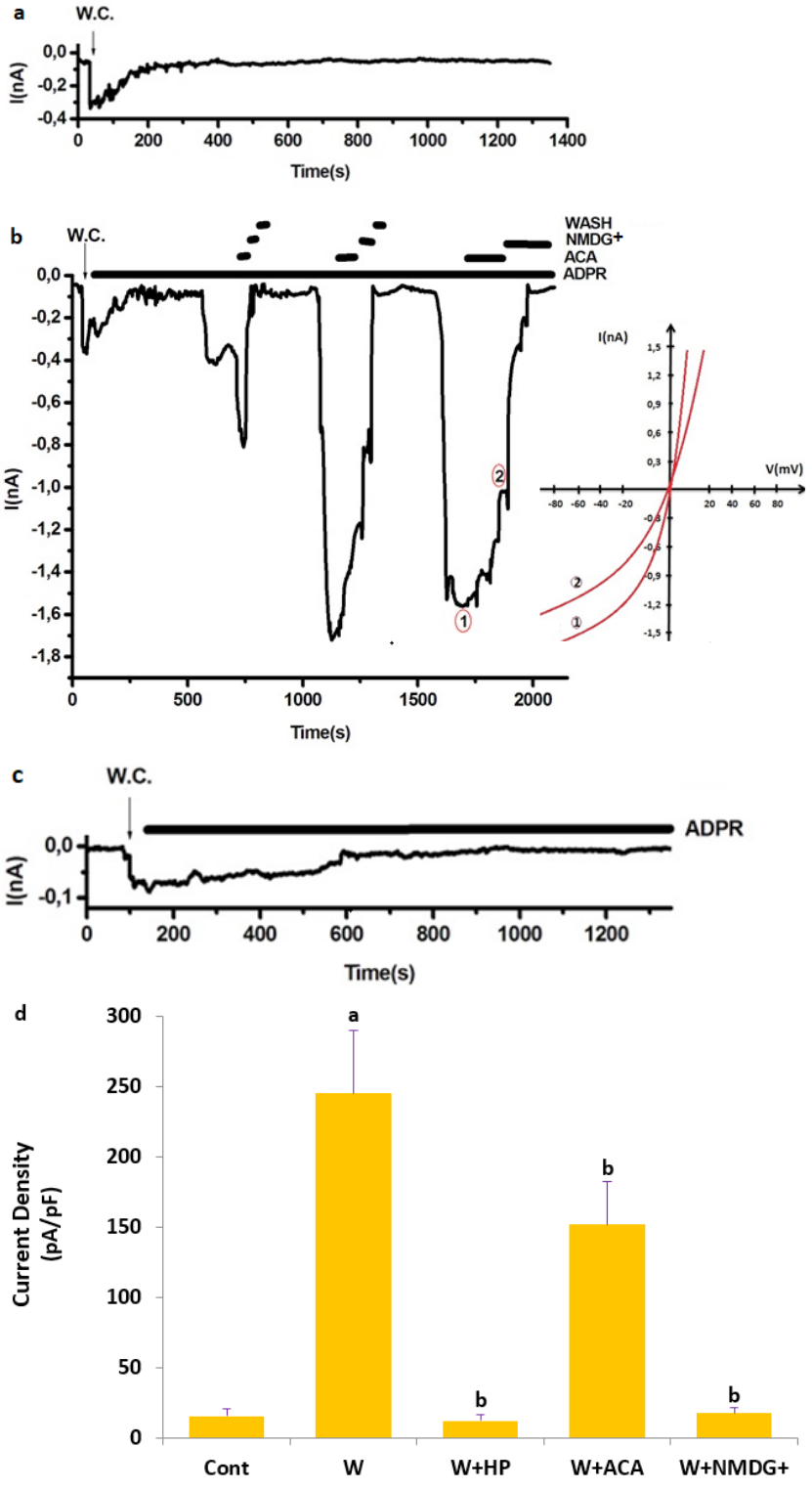

FIGURE 3. ***Hypericum perforatum*** **extract (HP) treatment reduced wound (W)-induced increase of TRPM2 current density in the MPK cells.** (n = 3 and mean ± SD). The TRPM2 currents in the cells were stimulated by intracellular ADPR (in the patch-pipette) (1 mM), although they were blocked by extracellular ACA (25 μM) and $NMDG^+$. W.C. is whole cell. (A) Control: Original recordings from control neuron. (B) W + ADPR group (without HP treatment). (C) W + HP group (with HP treatment). (D) TRPM2 channel current densities in the control (Cont), W, W + ACA and W + $NMDG^+$ groups. ($^a p \leq 0.001$ *vs.* control; $^b p \leq 0.001$ *vs.* W group).

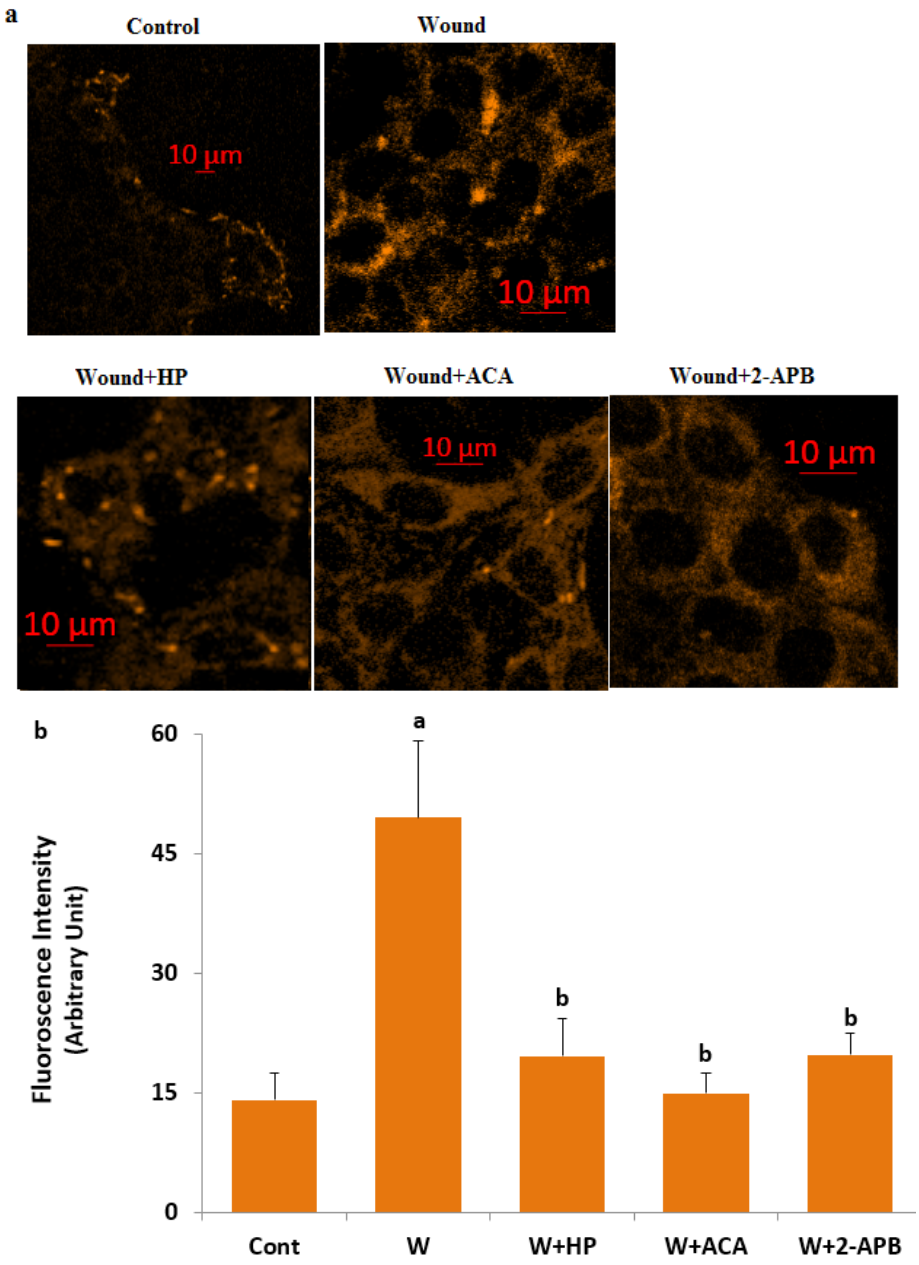

FIGURE 4. ***Hypericum perforatum*** **extract (HP) and TRPM2 channel blockers (ACA and 2-APB) decreased wound (W)-induced increase of mitochondrial membrane depolarization (MMP) in the MPK cells**. Control, wound (W), and W + HP (75 µM) cells were kept in the cell culture conditions for 72 h. Some cells in the W group were further incubated with ACA (25 µM) and 2-APB (100 µM) for 30 min. The cells were stained with JC-1 dye for 30 min and mean ± SD of fluorescence in 20 mm^2 of the neuron as arbitrary unit are presented; n = 15-20 independent experiments. The samples were analyzed by the laser confocal microscopy fitted with a 40X objective. (A) Images of the JC-1 fluorescence intensity in the five groups. Changes of the JC-1 fluorescence intensity in the five groups were also shown by columns (B). ($^a p \leq 0.001$ *vs.* control group; $^b p \leq 0.001$ *vs.* W group).

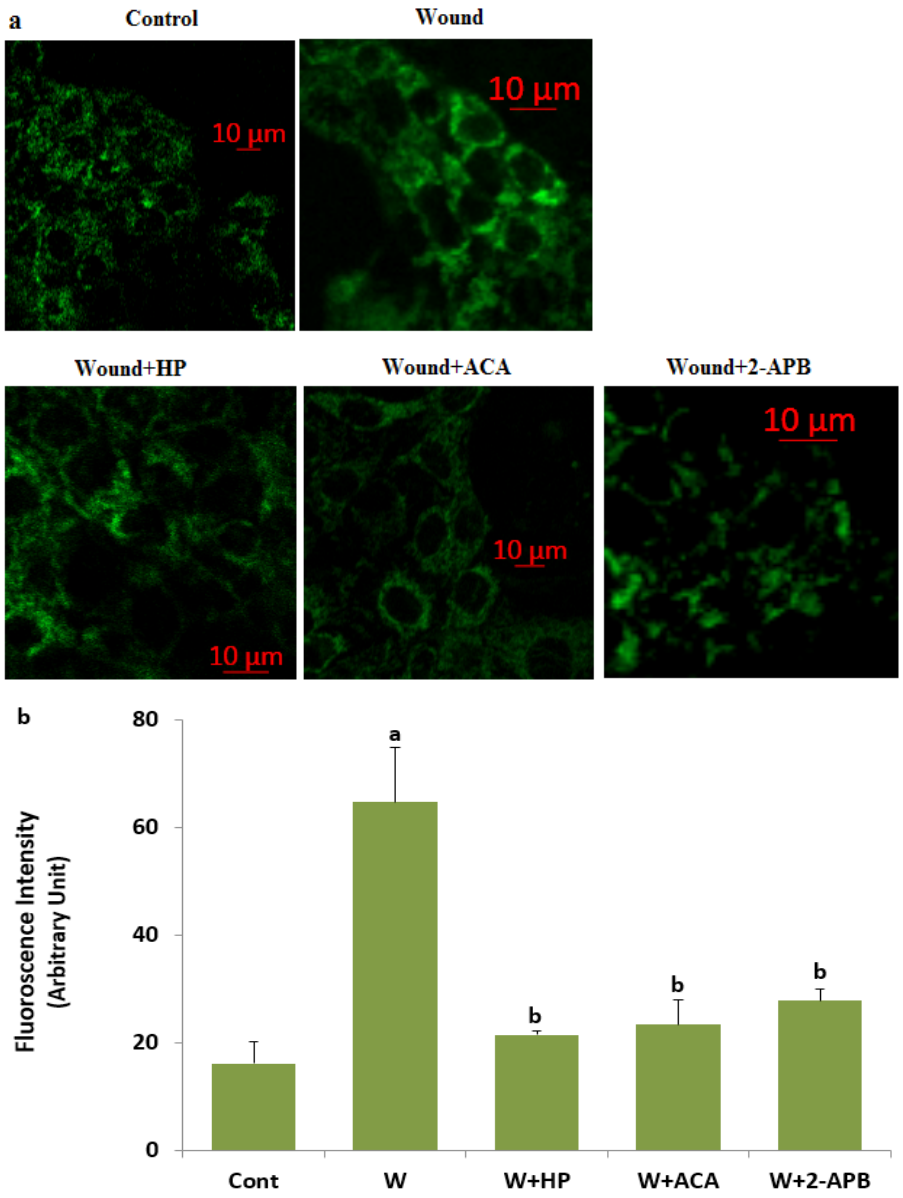

FIGURE 5. ***Hypericum perforatum extract*** **(HP) and TRPM2 channel blockers (ACA and 2-APB) modulated wound (W)-induced increase of intracellular ROS production in the MPK cells**. Control, wound (W), and W + HP (75 µM) cells were kept in the cell culture conditions for 72 h. Some cells in the W group were further incubated with ACA (25 µM) and 2-APB (100 µM) for 30 min. The cells were stained with DHR123 dye for 30 min and mean ± SD of fluorescence in 20 mm^2 of the neuron as arbitrary unit are presented; n = 15 - 20 independent experiments. The samples were analyzed by the laser confocal microscopy fitted with a 40X objective. (A) Images of the Rh123 fluorescence intensity in the five groups. Changes of the Rh123 fluorescence intensity in the five groups were also shown by columns (B). ($^{a}p \leq 0.001$ *vs.* control group; $^{b}p \leq 0.001$ *vs.* W group).

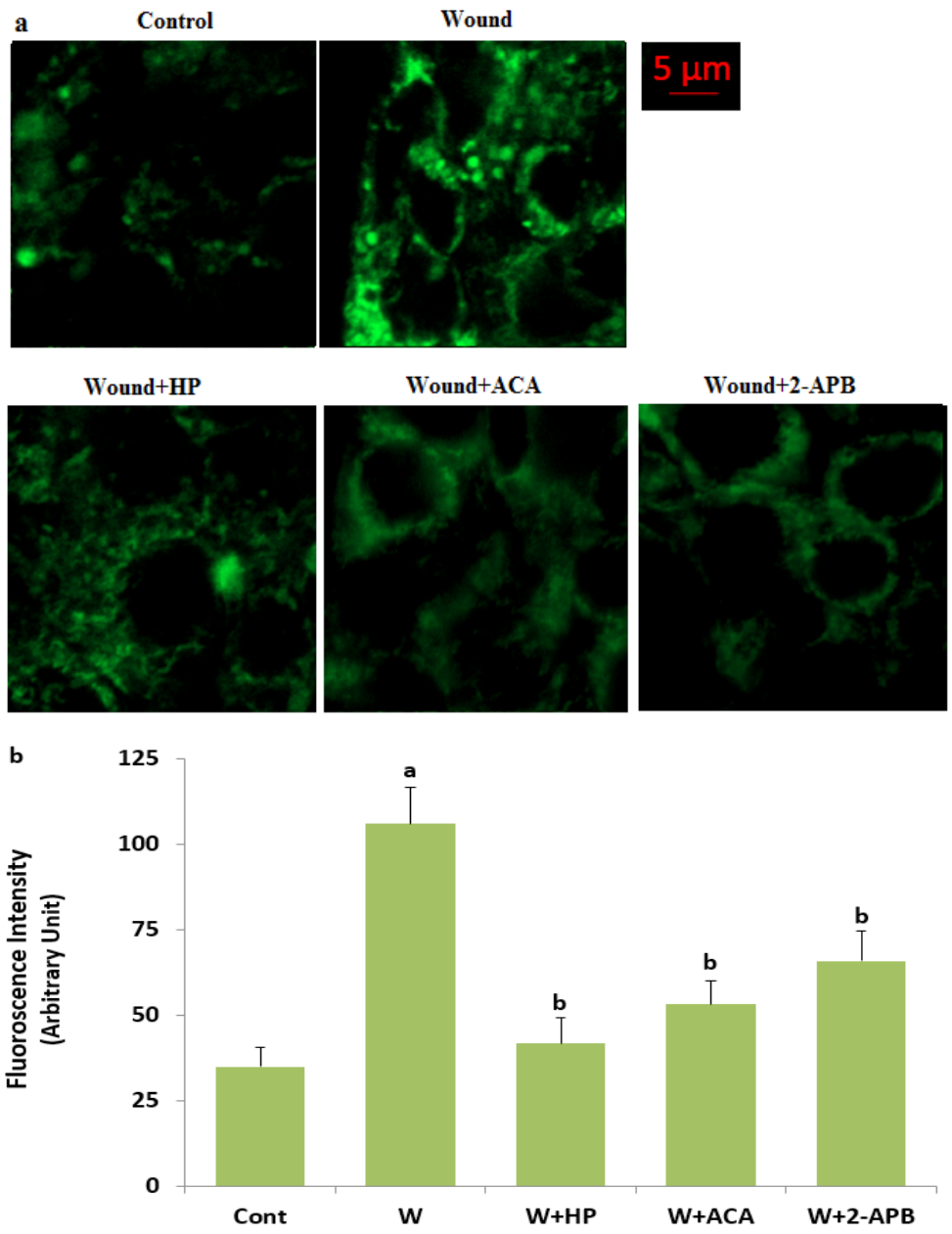

FIGURE 6. ***Hypericum perforatum*** **extract (HP) and TRPM2 channel blockers (ACA and 2-APB) diminished wound (W)-induced increase of early apoptosis (annexin V-FITC) level in the MPK cells**. Control, wound (W), and W + HP (75 µM) cells were kept in the cell culture conditions for 72 h. Some cells in the W group were further incubated with ACA (25 µM) and 2-APB (100 µM) for 30 min. The cells were stained with annexin V-FITC dye for 15 min and mean ± SD of fluorescence in 20 mm^2 of the neuron as arbitrary unit are presented; n = 15-20 independent experiments. The samples were analyzed by the laser confocal microscopy fitted with a 40X objective. (A) Images of the JC-1 fluorescence intensity in the five groups. Changes of the annexin V-FITC fluorescence intensity in the five groups were also shown by columns (B). ($^a p \leq 0.001$ *vs.* control group; $^b p \leq 0.001$ *vs.* W group).

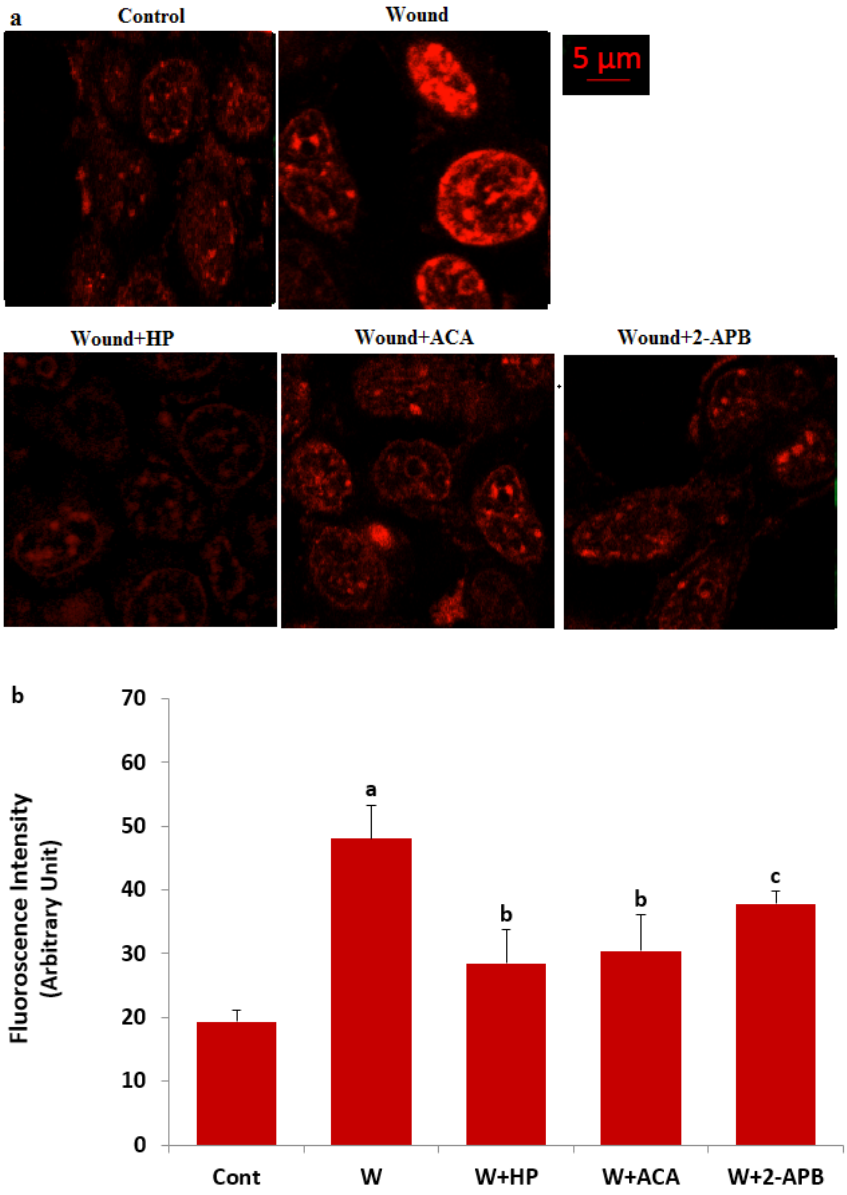

FIGURE 7. ***Hypericum perforatum*** **extract (HP) and TRPM2 channel blockers (ACA and 2-APB) reduced wound (W)-induced increase of late apoptosis (propidium iodide, PI) level in the MPK cells**. Control, wound (W), and W + HP (75 µM) cells were kept in the cell culture conditions for 72 h. Some cells in the W group were further incubated with ACA (25 µM) and 2-APB (100 µM) for 30 min. The cells were stained with PI dye for 15 min and mean ± SD of fluorescence in 20 mm^2 of the neuron as arbitrary unit are presented; n = 15 - 20 independent experiments. The samples were analyzed by the laser confocal microscopy fitted with a 40X objective. (A) Images of the PI fluorescence intensity in the five groups. Changes of the PI fluorescence intensity in the five groups were also shown by columns (B). ($^a p \leq 0.001$ *vs.* control group; $^b p \leq 0.001$ and $^c p \leq 0.05$ *vs.* W group).

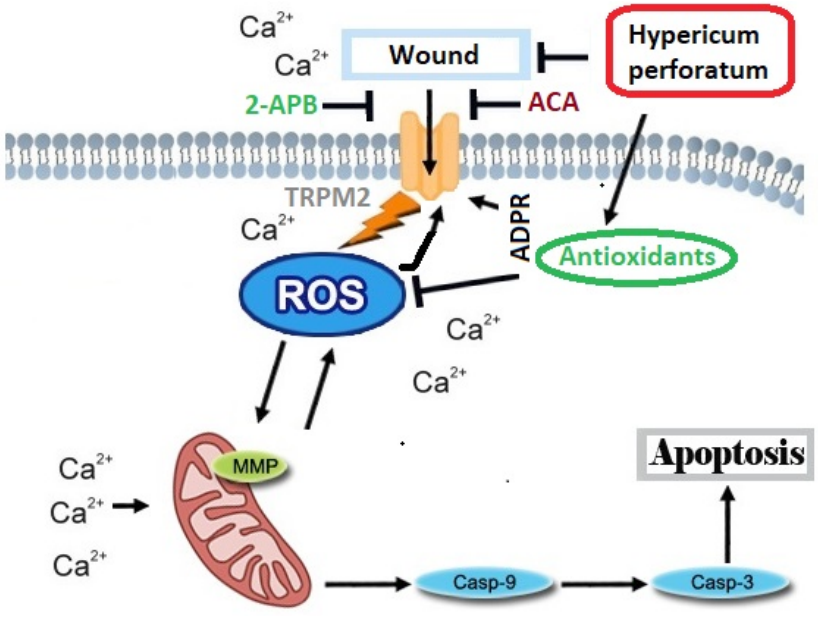

FIGURE 8. Graphical abstract of pathways involved in wound-induced apoptosis and reactive oxygen species (ROS) production and clearance by ***Hypericum perforatum*** **extract.** Wound can lead to the productions of several ROS from molecular oxygen. TRPM2 channel is activated by oxidative stress and ADP-ribose (ADPR), although it is inhibited by 2-APB and ACA. The main mechanism in the anti-apoptotic effect of *H. perforatum* is mediated by inhibition of ROS-mediated TRPM2 channel and caspase activations. Increase of mitochondrial membrane potential (MMP) through increase of cytosolic free Ca^{2+} concentration activates apoptosis factors and ROS from the mitochondria. In response, *H. perforatum* in the epithelial MPK cells stimulates antioxidant responses and inhibition of TRPM2 that facilitates the neutralization of ROS.

Results

HP modulates wound diameters dose dependently

In order to characterize the dose of HP in the MPK cells, morphological examinations were performed by using bride field laser confocal microscopy imaging. Injury diameters in the HP doses as zero, 5, 10, 25, 50, 75, 100, and 125 μM were 497, 395, 374, 307, 171, 185, 345, and 400, respectively (Fig. 1(A)). The HP treatment induced recovery effect on the wound diameters in the MPK cells. The wound diameter was lower in 5 and 10 μM groups than in zero groups ($p \leq 0.001$). In addition, the wound diameter was lower in 25 μM than in 5 and 10 μM groups ($p \leq 0.001$). The wound diameter was lowest in 50 and 75 μM groups ($p \leq 0.001$), and the recovery effect reached a plateau in the 50 and 75 μM doses (Fig. 1(B)). However, the wound healing diameters were increased in 100 and 125 μM doses and the doses of HP seem toxic for the cells. Therefore, we selected the 75 μM dose for future analyses.

Intracellular Ca^{2+} concentrations were diminished in the wound-induced MPK cells by the treatments of HP, ACA and 2-APB

After observation recovery changes in the wound, we suspected changes in the intracellular free Ca^{2+} concentration ($[Ca^{2+}]_i$) in the cells. Therefore, we investigated changes in Ca^{2+} concentration in the wound-induced cells after HP treatments (Fig. 2(a)). The fluorescence intensities of $[Ca^{2+}]_i$ were markedly higher in the wound group than in the control ($p \leq 0.001$) (Fig. 2(B)). However, the Ca^{2+} fluorescence intensities were decreased in the cell by the HP treatment and their intensities were significantly ($p \leq 0.001$) lower in the wound+HP group than in the wound group. The increase of Ca^{2+} fluorescence intensity in the wound groups was also prevented by the TRPM2 channel blockers (ACA and 2-APB), and their intensities were markedly lower in the wound + ACA and wound + 2-APB groups than in the wound group.

TRPM2 channel current densities were reduced in the wound-induced epithelial MPK cells by the treatments of HP and ACA

In addition to the laser confocal microscope analyses of $[Ca^{2+}]_i$ in the cells, we further investigated the involvement of TRPM2 channel in the increase of $[Ca^{2+}]_i$ in the cells. The cells were stimulated by intracellular ADPR (1 mM). There were no currents in the control (unstimulated) cells (Fig. 3(A)). However, the cells in the wound groups were gated by the ADPR stimulation, and the current densities were markedly ($p \leq 0.001$) higher in the wound group (245 pA/pF) than in the control (15 pA/pF) (Fig. 3(B)). However, the current densities were decreased by the treatment of ACA (25 μM) and $NMDG^+$, and they were markedly ($p \leq 0.001$) lower in the ACA and $NMDG^+$ groups than in the wound group. There was no current in the wound+HP group (Figs. 3(C) and 3(D)), although ADPR is present in the patch pipette ($p \leq 0.001$).

Wound injury-induced intracellular ROS production and MPP levels in the epithelial MPK cells were decreased by the HP and TRPM2 blocker treatments

After the observation increase of the concentration of $[Ca^{2+}]_i$ through TRPM2 activation in the MPK cells of the wound group, we decided to investigate changes in the MPP and ROS level changes by using fluorescent dyes (Figs. 4(A) and 5(A). The MPP (JC-1) (Fig. 4(B)) and ROS (DHR123) (Fig. 5(B)) levels were increased in the MPK cells by the wound induction ($p \leq 0.001$). The wound-induced increases of JC-1 and ROS levels were diminished by the HP, ACA, and 2-APB treatments.

Wound injury-induced early and late apoptosis levels in the epithelial MPK cells were diminished by the HP and TRPM2 blocker treatments

After the observation increase of the concentration of $[Ca^{2+}]_i$ through TRPM2 activation in the MPK cells of the wound group, we decided to investigate changes in the apoptosis level changes by using fluorescent dyes. The images of aV-FITC and PI were shown in Figs. 6(A) and 7(A), respectively. aV-FITC (Fig. 6) and PI (Fig. 7) fluorescence intensities were increased in the MPK cells by the wound induction ($p \leq 0.001$). However, the wound-induced early (aV-FITC) and late (PI) apoptosis levels were markedly (($p \leq 0.001$ and $p \leq 0.05$) diminished in the cells by the HP, ACA, and 2-APB treatments.

Discussion

The results of the present study indicated that the involvement of the TRPM2 channel on the wound-induced epithelial cell recover in the MPK cells. In addition, the decrease of mitochondrial oxidative stress, and apoptosis values were indicated by the HP results of the current study. To the date, there is no report on the values in the cells. Hence, the laser confocal microscopy and patch-clamp results are the novel pieces of evidence indicating the wound injury-induced apoptosis and oxidative neurotoxicity pathophysiological processes and implicating HP treatment on the TRPM2 in the epithelial cell wound recovery.

HP contains several antioxidant components such as flavonoids, hyperforin, and hypericin (Wölfle *et al*., 2014). HP stimulates the recovery of keratinocytes through inhibition of mitochondrial oxidative stress (Schmitt *et al*., 2006). The increase of MMP can occur as a result of an increase of $[Ca^{2+}]_i$ concentration (Nazıroğlu, 2012). The increased MPP levels induce result in intracellular ROS production levels (Carrasco *et al*., 2015; Almasi *et al*., 2019) (Fig. 8). However, the increased levels of MMP and ROS through inhibition of TRPM2 channels are diminished by the antioxidant properties of HP (Nazıroğlu *et al*., 2014a, 2014b and 2014c; Uslusoy *et al*., 2017). The wound injury exhibited a significant increase in the cellular MPP and ROS levels, as well as increased intracellular $[Ca^{2+}]_i$ concentration. HP treatment attenuated the TRPM2 channel activity, MPP and ROS levels, thereby decreasing $[Ca^{2+}]_i$ concentration and wound injury. These results suggest that HP treatment improves the wound-induced ROS and MPP in the epithelial MPK cells.

In the wound group, we observed increases of Ca^{2+} accumulation (Figs. 2(A) and 2(B)) and TRPM2 current density (Fig. 3(B)) in the MPK cells after oxidative stress (H_2O_2) and ADPR stimulations, respectively. However, there was no ADPR-induced Ca^{2+} accumulation and current in the MPK cells in the absence of ADPR (Fig. 3(A)) or presence of HP (Figs. 3(C) and 3(D)), consistent with HP being critical in inhibition of oxidative stress and ADPR-induced TRPM2 channel activation (Nazıroğlu *et al*., 2013; Özdemir

et al., 2016; Uslusoy *et al*., 2017; Jiang *et al*., 2018). Similar findings were made regarding the increase of mitochondrial oxidative stress through activation of TRPM2 (Figs. 4 and 5). Collectively, these results support the notion that the Ca^{2+} influx through TRPM2 channel activation plays an important role in the mitochondrial Ca^{2+} accumulation. A precedent was performed by a recent study indicating involvements of the TRPV1 and the Orai channel in cell migration and wound healing (Bastián-Eugenio *et al*., 2019). Similar to current results, the protective role of HP in rat sciatic nerve injury through inhibition of TRPM2 channels was reported (Uslusoy *et al*., 2017). Recently, it was reported that cutaneous wound healing is accelerated by mechanical stress, and treatment with hyperforin enhanced the acceleration through the facilitation of TRPC6 Ca^{2+} signaling in HaCaT human keratinocyte cells and neurons (Nazıroğlu, 2016; Takada *et al*., 2017). More recently, the involvement of 2-APB through inhibition of TRPV2 on hypertrophic scar formation and wound healing in cell culture of rat keratinocytes was also reported (Ishii *et al*., 2018).

An increase of MPP through excessive Ca^{2+} influx results in the increase of apoptosis level (Carrasco *et al*., 2015). The study further investigated the influence of HP treatment on apoptosis levels in the epithelial MPK cells. The apoptosis assay demonstrated that HP and TRPM2 channel blocker treatments could inhibit the early and late apoptosis levels in the cells. Thus, these results suggest that the wound injury-induced epithelial apoptosis contributes to the progression of cellular injury and then results in the reduction of injury recovery in MPK cells. However, HP treatment attenuated the apoptosis level in the cells. Similarly, it was reported that sciatic nerve wound healing capacities and brain oxidative injury of rats were increased through inhibition of mitochondrial oxidative stress and apoptosis level by the HP (Uslusoy *et al*., 2017; Uslusoy *et al*., 2019).

Taken together, our results suggest that the opening of the TRPM2 channel participates in the Ca^{2+} entry involved in the response of epithelial MPK cells to HP. The wound injury activated Ca^{2+} entry through activation of TRPM2 with mitochondrial depolarization, followed by the excessive production of ROS, subsequently leading to the apoptosis of the epithelial MPK cells. However, HP treatment has a valid effect on reducing wound formation in the cells by diminishing apoptosis and TRPM2 channel activity. The current results can indicate an interesting starting point for the development of new plant-based TRPM2 channel blockers on wound healing in cell culture and human skin.

Financial Disclosure

The study was supported by BSN Health, Analysis and Innovation Ltd. Inc. Teknokent, Isparta, Turkey (Project No: 2018-14). There is no financial disclosure of the current study.

Authors' Contributions

MN and FU formulated the present hypothesis and MN was responsible for writing the report. FU was responsible for preparing the cell culture. MN was responsible for the laser confocal microscope analyses.

Declaration of Conflicting Interests

All the authors have declared no conflict of interest in this article.

References

Adinolfi E, Callegari MG, Cirillo M, Pinton P, Giorgi C, Cavagna D, Rizzuto R, Di Virgilio F (2009). Expression of the $P2X_7$ receptor increases the Ca^{2+} content of the endoplasmic reticulum, activates NFATc1, and protects from apoptosis. *Journal of Biological Chemistry* **284**: 10120-10128.

Almasi S, Long CY, Sterea A, Clements DR, Gujar S, El Hiani Y (2019). TRPM2 silencing causes G2/M arrest and apoptosis in lung cancer cells via increasing intracellular ROS and RNS levels and activating the JNK pathway. *Cellular Physiology and Biochemistry* **52**: 742-757.

Altıparmak M, Eskitaşçıoğlu T (2018). Comparison of systemic and topical *Hypericum perforatum* on diabetic surgical wounds. *Journal of Investigative Surgery* **31**: 29-37.

Ashkani-Esfahani S, Hosseinabadi OK, Moezzi P, Moafpourian Y, Kardeh S, Rafiee S, Fatheazam R, Noorafshan A, Nadimi E, Mehrvarz S, Khoshneviszadeh M, Khoshneviszadeh M (2016). Verapamil, a calcium-channel blocker, improves the wound healing process in rats with excisional full-thickness skin wounds based on stereological parameters. *Advances in Skin and Wound Care* **29**: 271-274.

Bastián-Eugenio CE, Bohórquez-Hernández A, Pacheco J, Sampieri A, Asanov A, Ocelotl-Oviedo JP, Guerrero A, Darszon A, Vaca L (2019). Heterologous calcium-dependent inactivation of Orai1 by neighboring TRPV1 channels modulates cell migration and wound healing. *Communications Biology* **2**: 88.

Carrasco C, Rodríguez BA, Pariente JA (2015). Melatonin as a stabilizer of mitochondrial function: role in diseases and aging. *Turkish Journal of Biology* **39**: 822-831.

Caterina MJ, Pang Z (2016). TRP channels in skin biology and pathophysiology. *Pharmaceuticals (Basel)* **9**: E77.

Clapham DE (2003). TRP channels as cellular sensors. *Nature* **426**: 517-524.

Dubé J, Rochette-Drouin O, Lévesque P, Gauvin R, Roberge CJ, Auger FA, Goulet D, Bourdages M, Plante M, Moulin VJ, Germain L (2012). Human keratinocytes respond to direct current stimulation by increasing intracellular calcium: preferential response of poorly differentiated cells. *Journal of Cellular Physiology* **227**: 2660-2667.

Działo M, Mierziak J, Korzun U, Preisner M, Szopa J, Kulma A (2016). The potential of plant phenolics in prevention and therapy of skin disorders. *International Journal* of *Molecular Sciences* **17**: 160.

Ertilav K, Nazıroğlu M, Ataizi ZS, Braidy N (2019). Selenium enhances the apoptotic efficacy of docetaxel through activation of TRPM2 channel in DBTRG glioblastoma cells. *Neurotoxicity Research* **35**: 797-808.

Hara Y, Wakamori M, Ishii M, Maeno E, Nishida M, Yoshida T, Yamada H, Shimizu S, Mori E, Kudoh J, Shimizu N, Kurose H, Okada Y, Imoto K, Mori Y (2002). LTRPC2 Ca^{2+}-permeable channel activated by changes in redox status confers susceptibility to cell death. *Molecular Cell* **9**: 163-173.

Ishii T, Uchida K, Hata S, Hatta M, Kita T, Miyake Y, Okamura K, Tamaoki S, Ishikawa H, Yamazaki J (2018). TRPV2

channel inhibitors attenuate fibroblast differentiation and contraction mediated by keratinocyte-derived TGF-β1 in an in vitro wound healing model of rats. *Journal of Dermatological Science* **90**: 332-342.

Jiang LH, Li X, Syed Mortadza SA, Lovatt M, Yang W (2018). The TRPM2 channel nexus from oxidative damage to Alzheimer's pathologies: an emerging novel intervention target for age-related dementia. *Ageing Research Reviews* **47**: 67-79.

Joshi DC, Bakowska JC (2011). Determination of mitochondrial membrane potential and reactive oxygen species in live rat cortical neurons. *Journal of Visualized Experiments* **51**: 2704.

Kang P, Zhang W, Chen X, Yi X, Song P, Chang Y, Zhang S, Gao T, Li C, Li S (2018). TRPM2 mediates mitochondria-dependent apoptosis of melanocytes under oxidative stress. *Free Radical in Biology and Medicine* **126**: 259-268.

Keil VC, Funke F, Zeug A, Schild D, Müller M (2011). Ratiometric high-resolution imaging of JC-1 fluorescence reveals the subcellular heterogeneity of astrocytic mitochondria. *Pflügers Archiv-European Journal of Physiology* **462**: 693-708.

Lee Y, Kim MT, Rhodes G, Sack K, Son SJ, Rich CB, Kolachalama VB, Gabel CV, Trinkaus-Randall V (2019). Sustained Ca^{2+} mobilizations: a quantitative approach to predict their importance in cell-cell communication and wound healing. *PLoS One* **14**: e0213422.

Li X, Wu G, Han F, Wang K, Bai X, Jia Y, Li Z, Cai W, Zhang W, Su L, Hu D (2019). SIRT1 activation promotes angiogenesis in diabetic wounds by protecting endothelial cells against oxidative stress. *Archives of Biochemistry* and *Biophysics* **661**: 117-124.

Liu CX, Tan YR, Xiang Y, Liu C, Liu XA, Qin XQ (2018). Hydrogen sulfide protects against chemical hypoxia-induced injury via attenuation of ROS-mediated Ca^{2+} overload and mitochondrial dysfunction in human bronchial epithelial cells. *BioMed Research International* **2018**: 2070971.

McHugh D, Flemming R, Xu SZ, Perraud AL, Beech DJ (2003). Critical intracellular Ca^{2+} dependence of transient receptor potential melastatin 2 (TRPM2) cation channel activation. *Journal of Biological Chemistry* **278**: 11002-11006.

Nazıroğlu M, Çiğ B, Özgül C (2014b). Modulation of oxidative stress and Ca^{2+} mobilization through TRPM2 channels in rat dorsal root ganglion neuron by *Hypericum perforatum*. *Neuroscience* **263**: 27-35.

Nazıroğlu M, Çiğ B, Yazğan Y, Schwaerzer GK, Theilig F, Pecze L (2019). Albumin evokes Ca^{2+}-induced cell oxidative stress and apoptosis through TRPM2 channel in renal collecting duct cells reduced by curcumin. *Scientific Reports* **9**: 12403.

Nazıroğlu M, Kutluhan S, Ovey IS, Aykur M, Yurekli VA (2014a). Modulation of oxidative stress, apoptosis, and calcium entry in leukocytes of patients with multiple sclerosis by *Hypericum perforatum*. *Nutritional Neuroscience* **17**: 214-221.

Nazıroğlu M, Lückhoff A (2008). A calcium influx pathway regulated separately by oxidative stress and ADP-Ribose in TRPM2 channels: single channel events. *Neurochemical Research* **33**: 1256-1262.

Nazıroğlu M, Sahin M, Ciğ B, Aykur M, Erturan I, Ugan Y (2014c). *Hypericum perforatum* modulates apoptosis and calcium mobilization through voltage-gated and TRPM2 calcium channels in neutrophil of patients with Behcet's disease. *Journal of Membrane Biology* **247**: 253-262.

Nazıroğlu M, Uğuz AC, Ismailoğlu Ö, Çiğ B, Özgül C, Borcak M (2013). Role of TRPM2 cation channels in dorsal root ganglion of rats after experimental spinal cord injury. *Muscle Nerve* **48**: 945-950.

Nazıroğlu M (2012). Molecular role of catalase on oxidative stress-induced Ca^{2+} signaling and TRP cation channel activation in nervous system. *Journal of Receptors and Signal Transduction* **32**: 134-141.

Nazıroğlu M (2016). Is *Hypericum perforatum* agonist or antagonist of TRPC6 in neurons? *Journal of Cellular Neuroscience and Oxidative Stress* **8**: 595-600.

Oliveira AI, Pinho C, Sarmento B, Dias AC (2016). Neuroprotective activity of *Hypericum perforatum* and its major components. *Frontiers in Plant Science* **7**: 1004.

Oz A, Celik O, Ovey IS (2017). Effects of different doses of curcumin on apoptosis, mitochondrial oxidative stress and calcium influx in DBTRG glioblastoma cells. *Journal of Cellular Neuroscience and Oxidative Stress* **9**: 617-629.

Özdemir ÜS, Nazıroğlu M, Şenol N, Ghazizadeh V (2016). *Hypericum perforatum* attenuates spinal cord injury-induced oxidative stress and apoptosis in the dorsal root ganglion of rats: involvement of TRPM2 and TRPV1 channels. *Molecular Neurobiology* **53**: 3540-3551.

Pariente R, Bejarano I, Rodríguez AB, Pariente JA, Espino J (2018). Melatonin increases the effect of 5-fluorouracil-based chemotherapy in human colorectal adenocarcinoma cells in vitro. *Molecular and Cellular Biochemistry* **440**: 43-51.

Polzin D, Kaminski HJ, Kastner C, Wang W, Krämer S, Gambaryan S, Russwurm M, Peters H, Wu Q, Vandewalle A, Bachmann S, Theilig F (2010). Decreased renal corin expression contributes to sodium retention in proteinuric kidney diseases. *Kidney International* **78**: 650-659.

Schmitt LA, Liu Y, Murphy PA, Petrich JW, Dixon PM, Birt DF (2006). Reduction in hypericin-induced phototoxicity by *Hypericum perforatum* extracts and pure compounds. *Journal of Photochemistry and Photobiology B* **85**: 118-130.

Takada H, Yonekawa J, Matsumoto M, Furuya K, Sokabe M (2017). Hyperforin/HP-β-Cyclodextrin enhances mechanosensitive Ca^{2+} signaling in HaCaT keratinocytes and in atopic skin ex vivo which accelerates wound healing. *BioMed Research International* **2017**: 8701801.

Uslusoy F, Nazıroğlu M, Çiğ B (2017). Inhibition of the TRPM2 and TRPV1 channels through *Hypericum perforatum* in sciatic nerve injury-induced rats demonstrates their key role in apoptosis and mitochondrial oxidative stress of sciatic nerve and dorsal root ganglion. *Frontiers in Physiology* **8**: 335.

Uslusoy F, Nazıroğlu M, Övey İS, Sönmez TT (2019). *Hypericum perforatum* L. supplementation protects sciatic nerve injury-induced apoptotic, inflammatory and oxidative damage to muscle, blood and brain in rats. *Journal of Pharmacy and Pharmacology* **71**: 83-92.

Vafi F, Bahramsoltani R, Abdollahi M, Manayi A, Hossein Abdolghaffari A, Samadi N, Amin G, Hassanzadeh G, Jamalifar H, Baeeri M, Heidari M, Khanavi M (2016). Burn wound healing activity of *Lythrum salicaria* L. and *Hypericum scabrum* L. *Wounds* **2016**: WNDS20160929-2.

Wölfle U, Seelinger G, Schempp CM (2014). Topical application of St. John's wort (*Hypericum perforatum*). *Planta Medicine* **80**: 109-120.

Yin J, Xu K, Zhang J, Kumar A, Yu F-SX (2007). Wound-induced ATP release and EGF receptor activation in epithelial cells. *Journal of Cell Science* **120**: 815-825.